Surface melting of multilayer oxygen films on graphite studied by neutron diffraction

R. Chiarello, J. P. Coulomb,* J. Krim, and C. L. Wang
Department of Physics, Northeastern University, Boston, Massachusetts 02115
(Received 9 November 1987; revised manuscript received 23 May 1988)

The results of a neutron-diffraction study of the melting properties of multilayer oxygen films are presented. The experiments have been carried out between 30 and 55 K on films ranging from 2 to 8 layers in thickness. A compound solid-liquid film is observed in the range 40–48 K. This composite film results from surface melting of the solid film phase which is present at 40 K. The thickness of its melted component is proportional to $\ln(T_t - T)$, where T_t is the melting temperature of bulk oxygen. The structure of its solid component is nearly identical to that of the bulk β phase. The data suggest that multiple wetting transitions may be present in this system.

I. INTRODUCTION

Thin films adsorbed on solid substrates frequently exhibit physical properties consistent with those predicted for two-dimensional (2D) rather than three-dimensional (3D) systems.[1] The melting temperature of a single-layer film is one such property, and is generally observed to be much lower than that of the corresponding bulk material.[2] Consider a film which is two or three layers thick: Will its melting temperature fall monotonically between that of the 2D monolayer and the 3D bulk melting point? With this motivation, we have carried out a neutron-diffraction study of the melting properties of multilayer oxygen films adsorbed on graphite.

Of the many systems we might have selected for such a study, oxygen on graphite was chosen on the basis of experimental convenience and the extensive literature available on monolayer and multilayer oxygen films.[3–13]

Figure 1 shows the phase diagram for this system based on Refs. 3–13 and the present work. Surface coverage is expressed in units of molecules per square angstrom (molecules/Å^2). Below 39 K, oxygen exhibits a variety of solid film phases. Monolayer solids (0.7–0.11 molecules/Å^2) melt in the temperature range 32–39 K, well below the 3D melting point, $T_t = 54.4$ K. Below 25 K these films do not grow arbitrarily thick as more oxygen condenses on the surface. Instead, as surface coverage is raised beyond about 0.25 molecules/Å^2 (2–3 molecular layers), the oxygen forms 3D crystallites which coexist with the film.[14] As temperature increases beyond 48 K, progressively thicker films are able to form, and a wetting transition occurs at the bulk solid-liquid melting point. We will present evidence here that a second wetting transition may be present, associated with the bulk β-solid–γ-solid triple point.

Film fluid phases are observed below T_t over a wide range of surface coverage. The "fluid film" phase occurring above 48 K is similar to bulk liquid oxygen. In a Letter we reported the "fluid II" phase to be a compound solid-liquid phase which can be attributed to surface melting of the 2D solid.[15] We now report in detail the structure of the multilayer oxygen film as it melts, evolving from 2D solid to fluid film via the surface-melted phase.

II. SURFACE MELTING AND TRIPLE POINT WETTING

Surface melting is in principle a widespread phenomenon consisting of the formation of a stable layer of liquid which wets a solid-vapor interface at temperatures below the triple point. Recent experiments have demonstrated the existence of surface melting in bulk crystals[16] and in adsorbed films.[17,18] The theory of surface melting of bulk matter[19–21] is relevant to the case of films and can be summarized as follows.

The surface free energy F_s of a bulk solid-vapor interface [Fig. 2(a)] is

$$F_s = \gamma_{sv} A \ , \tag{1}$$

where γ_{sv} is the surface tension of the solid-vapor interface and A is its area. If the liquid wets the solid surface,

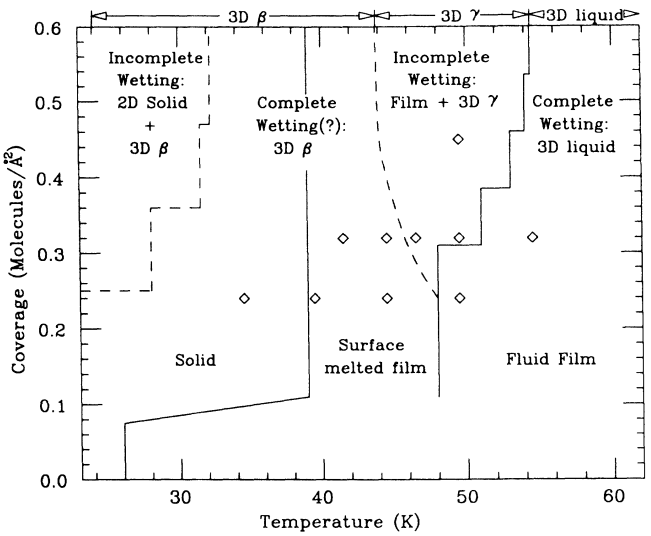

FIG. 1. Proposed phase diagram for oxygen on graphite (Refs. 3–13 and this work). Diamonds represent data points of this study. The dashed lines represent boundaries whose exact locations have yet to be determined. The "surface-melted" film has been referred to as the "fluid II" phase in previous publications (Refs. 3 and 15).

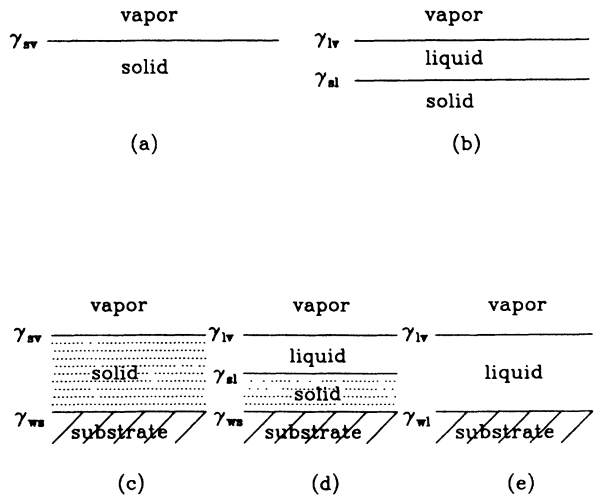

FIG. 2. Schematic of surface melting for bulk solids [(a) and (b)] and solid films [(c)–(e)].

i.e., if $\gamma_{sv} > (\gamma_{sl}+\gamma_{lv})$, then the surface free energy will be lowered by the creation of a thin slab of liquid [Fig. 2(b)] and the decrease in surface free energy δF_s will be

$$\delta F_s = (\gamma_{sl}+\gamma_{lv}-\gamma_{sv})A \ , \tag{2}$$

where γ_{sl} and γ_{lv} are the surface tensions of the solid-liquid and liquid vapor interfaces. Minimization of the total change in free energy

$$\delta F = \delta F_s + \delta F_m \tag{3}$$

will determine the thickness of the liquid slab d_l at any given temperature. Here, δF_m is the increase in free energy of the system due to melting a portion of the solid to form the liquid slab. The temperature dependence of d_l arises from δF_m which is zero at T_t and increases at lower T. For van der Waals solids with long-range interactions, one obtains $d_l \sim (T_t - T)^{-1/3}$, whereas for solids modeled by short-range interactions $d_l \sim \ln(T_t - T)$.[22,23]

Surface melting of an adsorbed film on a solid substrate is somewhat more complicated on account of the additional surface tension γ_{ws} arising from the film-substrate interface. The surface tension of the substrate-solid film-vapor interface $(\gamma_{ws}+\gamma_{sv})$ [Fig. 2(c)] must now be compared to both that of a surface-melted film $(\gamma_{ws}+\gamma_{sl}+\gamma_{lv})$ [Fig. 2(d)] and that of a completely liquid film $(\gamma_{wl}+\gamma_{lv})$ [Fig. 2(e)].

Pandit and Fisher[24] have employed such considerations for adsorbed films near bulk triple points and present a wide variety of scenarios which may occur, many of which include film surface melting. Moreover, they stress the inseparable relationship between film melting and wetting properties near bulk triple points. If the liquid film is able to lower the surface free energy more than the solid film, it is said to wet the substrate "more strongly" than the solid. The liquid will then remain the stable film phase to some finite temperature below the bulk triple point, preventing complete wetting of the substrate by the solid. As temperature increases, a transition from incomplete wetting (by the bulk solid) to complete wetting (by the bulk liquid) will occur at T_t. Ebner[25] has modeled this transition as a Potts lattice gas and has obtained mean-field predictions for the phase diagrams of multilayer films near triple points. Essentially all experimentally observed wetting transitions observed to date occur at bulk triple points,[26–28] oxygen on graphite being no exception. It is interesting to note, however, that a second triple point exists at 43.8 K corresponding to the phase transition between the 3D solid γ phase of oxygen (stable between 43.8 and 54.4 K) and the 3D solid β phase. The existence of a triple point wetting transition at 54.4 K indicates that liquid oxygen wets graphite more strongly than γ oxygen. In what follows we will argue that *both* liquid and β oxygen wet more strongly than γ oxygen, and as a consequence multiple wetting transitions may occur in this system.

III. MULTILAYER LINE SHAPES

Our analysis of the diffraction line shapes follows that previously described in Kjems *et al.*[29] and Larese *et al.*[30] Multilayer line shapes were obtained by assuming the surface monolayer line shape is modified by a structure factor. The structure factor describes multilayer interference effects, and for a given (hk) Bragg reflection is

$$F_{hk} = \sum_j b_j \exp[-2\pi i(hx_j + ky_j + cQ_z z_j)] \ , \tag{4}$$

where b_j is the coherent scattering amplitude of the jth atom in the unit cell; x_j, y_j, and z_j are reduced positional coordinates; Q_z is the z component of the scattering wave vector Q relative to a coordinate system fixed on a given crystallite, and c is the interlayer spacing. The ordered arrangement of molecules of the adsorbed layers determines the characteristic shape of the multilayer diffraction pattern. For triangular structures, and considering only the (10) Bragg reflection, the following expressions are obtained from Eq. (4):[29,30]

$$|F_{\langle 10\rangle}|^2 = 2-\cos(cQ_z) \ , \tag{5}$$

$$|F_{\langle 10\rangle}|^2 = 3-2\cos(cQ_z)+2\cos(2cQ_z) \ , \tag{6}$$

$$|F_{\langle 10\rangle}|^2 = 3-2\cos(2cQ_z)-\cos(cQ_z) \ , \tag{7}$$

for the scattering from an AB bilayer, ABA trilayer, and ABC trilayer, respectively.

For surface monolayers of spherically symmetric molecules, the z component of the structure factor does not enter the problem. However, for diatomic molecules oriented perpendicular to the crystallite surface, the surface monolayer may be characterized as a bilayer with AA stacking. The interplanar separation is the molecular bond length. For an AA bilayer the following expression is obtained from Eq. (4):

$$|F_{\langle 10\rangle}|^2 \sim \cos^2(\tfrac{1}{2}Q_z l) \ , \tag{8}$$

where l is the molecular bond length. We have included this term in our determination of surface monolayer and multilayer line shapes for molecules perpendicular to the surface, assuming a bond length $l = 1.208$ Å.[31] If the dia-

tomic molecule is oriented parallel to the 2D crystallite of the substrate, then the z component of the structure factor does not enter the problem.

The substrate for this experiment (Papyex exfoliated graphite) has basal planes with a preferred orientational distribution. The determination of the preferred orientational distribution of the basal planes and the method used to determine surface monolayer line shapes are described in detail elsewhere.[32,33]

IV. EXPERIMENTAL DETAILS

The neutron scattering measurements were performed at Grenoble's Institut Laue-Langevin on the D1b beam line operating in the elastic mode. The wavelength of the incident neutrons was 2.517 Å. Elastically scattered neutrons were collected within the range 0.87–2.86 $Å^{-1}$. The overlayer diffraction patterns were obtained by subtracting off the background due to the bare graphite. The substrate consisted of 1.36 gm of Papyex exfoliated graphite, density 0.1 g/cm^3 and having a surface area estimated to be 36 m^2/g. This sample was roughly one tenth as dense as that ordinarily employed in diffraction studies so as to minimize condensation of oxygen into capillaries and crevices. The substrate was loaded in an aluminum sample can within a helium-flow cryostat so that the plane of scattering was parallel to the planes of the graphite disks, corresponding to the average basal plane orientation of the crystallites. Surface coverage was calibrated with respect to that of a $(\sqrt{3}\times\sqrt{3})$ registered monolayer phase (0.064 molecules/$Å^2$) of methane. The oxygen was condensed at 55 K and then slowly cooled to the temperature of interest. Surface coverage corrections due to changes in the oxygen vapor pressure with temperature were on the order of one-hundredth to one-thousandth of a monolayer, and were neglected. Annealing after cooling produced no change in the observed diffraction scans. Our measurements were carried out between 34.5 and 54.5 K, and for coverages ranging from 0.24 to 0.9 molecules/$Å^2$, the equivalent of two to eight solid layers (density 0.11 molecules/$Å^2$) or three to twelve liquid layers (density 0.075 molecules/$Å^2$).

V. EXPERIMENTAL RESULTS

Figure 3 shows scans carried out at surface coverages of 0.32 molecules/$Å^2$. The scan at 49.5 K has been recorded in the fluid film plus 3D γ regime of Fig. 1, well below the bulk triple point. The scans between 41.5 and 46.5 K have been recorded in the surface-melted film regime. All of the surface-melted film scans show evidence of a compound film phase, indicated by the superposition of solidlike peaks with a fluid film background. We previously argued that the surface-melted regime results from surface melting of the 2D solid phases.[15] We now report in detail our structural determination of the O_2 film as it melts.

The scattering intensity at $Q=2.0$ $Å^{-1}$ is due only to the fluid film phase and is well away from any film or 3D solid peak. We employ the intensity at this point to estimate the quantity of fluid film present in each of the surface-melted film scans, and list this as n_l in Table I.

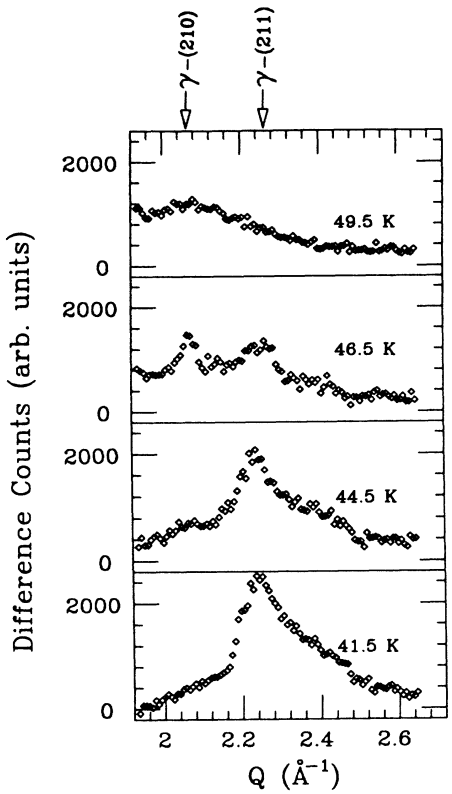

FIG. 3. Diffraction scans recorded at surface coverage 0.32 molecules/$Å^2$. Bulk γ peaks are observed at $T=46.5$ K. Too little of the bulk γ phase is present at 49.5 K to be observed in the diffraction scan.

We then subtract the fluid film portion (via direct numerical subtraction of fractions of the 49.5 K scan) from each surface-melted film scan so as to reveal the line shape of the solid component. The resulting scans, including our best fit, are shown in Fig. 4. For reference, we also include a scan recorded in the 2D solid regime at 0.24 molecules/$Å^2$ and 34.5 K [Fig. 4(b)]. The quantity of solid present, $n_s=n-n_l$, is listed in Table I in units of molecules/$Å^2$ and layers (0.11 molecules/$Å^2$ per layer), and can be compared to the thickness of the solid layer, n_s (layers:fit), as determined by the best fit to the data.

To fit the multilayer diffraction data it was necessary to model the ordered stacking arrangement of the adsorbed O_2 molecules. The ordered stacking arrangement of the molecules determines the characteristic shape of the multilayer line shape through the structure factor, as outlined in Sec. III.

A solid film which is exactly one, two, or three layers thick may be modeled by pure monolayer, pure bilayer (AB, AA stacking), or pure trilayer (ABA, ABC stacking) line shapes. A linear combination of pure stacking line shapes is needed to fit the data recorded at noninteger thicknesses. For example, a film between two and three layers thick will have a certain number of molecules ordered in an AB stacking arrangement with the remaining molecules ordered in an ABC or ABA stacking arrangement. The film is best modeled by forming the total

TABLE I. Film characteristics in the surface melting regime.

n (molecules/Å^2)	0.24	0.24	0.24	0.32	0.32	0.32
T (K)	34.5	39.5	44.5	41.5	44.5	46.5
n_l (molecules/Å^2)	0	0.015	0.165	0.062	0.145	0.24
n_s (molecules/Å^2)	0.24	0.225	0.075	0.258	0.175	0.08
n_s (layers)	2.18	2.05	0.68	2.34	1.59	0.73
n_s (layers:fit)	2.19	2.17	0.75	2.22	1.66	a
A (%)			100		25	a
a_A;L (Å)			3.29;42		3.21;24	a
AB (%)	74	76		70	75	a
a_{AB};L (Å)	3.31;70	3.31;59		3.30;78	3.29;55	a
ABC (%)	26	24		30		a
a_{ABC};L (Å)	3.29;77	3.29;66		3.29;66		a
a_{nn} (β solid) (Å)	3.295	3.322	3.34	3.34	3.33	b
c (Å)	3.88	3.90		3.88	3.6	a
P/P_0[c]	0.77	0.78	0.85	0.79	0.87	0.95

[a]Data not fit.
[b]β oxygen not stable at this temperature.
[c]Estimate.

multilayer line shape as a linear combination of the two pure stacking line shapes. For a film consisting of AB ordered sections plus ABC ordered sections the total multilayer line shape is represented by

$$f_{AB}\,AB + f_{ABC}\,ABC\ , \tag{9}$$

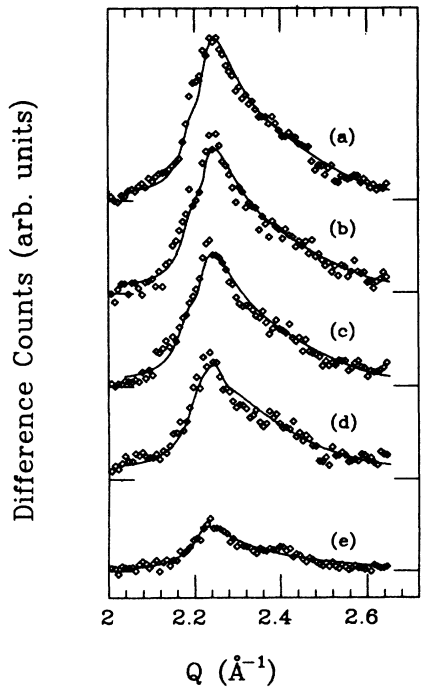

FIG. 4. Diffraction scans of the solid component of the surface-melted film along with the best fit to the data. (a) 0.32 molecules/Å^2 at 41.5 K (liquid subtracted), $n_s=2.3$ layers; (b) 0.24 molecules/Å^2 at 34.5 K (ζ solid regime), $n_s=2.2$ layers; (c) 0.24 molecules/Å^2 at 39.5 K (liquid subtracted), $n_s=2.1$ layers; (d) 0.32 molecules/Å^2 at 44.5 K (liquid subtracted), $n_s=1.6$ layers; (e) 0.24 molecules/Å^2 at 44.5 K (liquid subtracted), $n_s=0.7$ layers.

where the coefficients f_{AB} and f_{ABC} are the respective fractions of molecules included in the AB and ABC ordered sections. AB represents the calculated multilayer line shape for pure AB stacking of the molecules, and ABC represents the calculated multilayer line shape for pure ABC stacking. The coefficients are subject to the condition $f_{AB}+f_{ABC}=1$.

Similarly, solid films between one and two layers may be divided into monolayer plus AB bilayer sections. The total line shape of this film is represented by

$$f_A\,A + f_{AB}\,AB\ , \tag{10}$$

where the coefficients f_A and f_{AB} are the respective fractions of molecules in the monolayer and AB bilayer sections.

We began fitting the multilayer diffraction data by assuming pure bilayer (AB, AA stacking) and pure trilayer (ABA, ABC stacking) line shapes. For each line shape we also modeled the O_2 molecules oriented either all parallel or all perpendicular to the substrate, and allowed the molecules within a plane to be arranged in either equilateral or isosceles triangles.

The best fits to the data were obtained with total multilayer line shapes of monolayer plus pure AB stacking line shapes for a film of approximately 1.7 solid layers, and AB plus ABC line shapes for films between two and three solid layers. The best fit corresponded to O_2 molecules oriented perpendicular to the substrate and arranged in equilateral triangles within the planes. f_A and f_{AB} (f_{AB} and f_{ABC}) were treated as parameters in the fitting routine. Other fitting parameters included the coherence length L, nearest-neighbor spacing a_A, a_{AB}, or a_{ABC}, interlayer spacing c, and normalized intensity. The interlayer spacing was varied for each type of stacking, but was assumed constant between layers of a given type of stacking.

The best fit parameters are listed in Table I. Throughout the surface melting regime, the solid component of the film is growing in an ABC stacking ar-

rangement with lattice parameters quite close to that of the 3D β phase of oxygen. This rhombohedral phase is stable between 24 and 43.8 K and consists of an *ABC* stacking arrangement with 3.76 Å between the individual planes of molecules.[34] As the temperature is increased from 40 to 48 K, the quantity of liquid increases. Assuming the liquid density to be 0.075 molecules/Å^2 per layer, the surface-melted liquid layer thickness n_l is well described by

$$n_l = 12.9 - 4.70 \ln(54.4 - T) . \quad (11)$$

Figure 5(a) shows the number of liquid layers for coverages of 0.24 molecules/Å^2 (diamonds) and 0.32 molecules/Å^2 (squares) along with our best fit to the data, Eq. (11). The cross at 48±1 K and four liquid layers corresponds to the "feature" reported in heat-capacity studies[4,6] at 47 K and microbalance studies[9] at 49 K. We associate this feature with the high-temperature limit of the surface melting regime. Our diffraction results place this upper limit in the range $46.5 < T < 49.5$ K. The maximum film thickness in this temperature range is known to be four layers.[10] The cross at 39±1 K and 0 liquid layers corresponds to the low-temperature limit of the "fluid II" regime reported in x-ray diffraction studies.[3] Our results place this lower limit to the surface melting regime in the range $34.5 < T < 39.5$ K.

In Fig. 5(b) $\ln(n_l)$ is plotted as a function of $\ln(T_t - T)$.

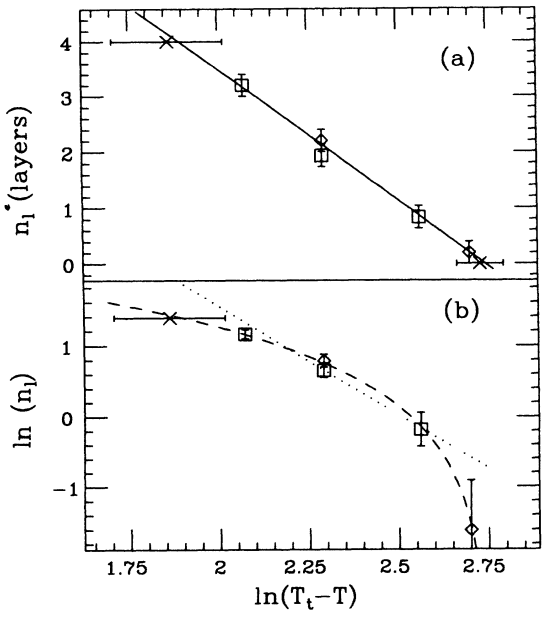

FIG. 5. (a) Number of liquid layers as a function of $\ln(T_t - T)$ for coverages of 0.24 molecules/Å^2 (diamonds) and 0.32 molecules/Å^2 (squares) layers. The solid line corresponds to the best logarithmic fit to the data, Eq. (11). Crosses denote the beginning and end of the surface-melted regime, as determined in previous studies (see the text) (Refs. 4, 6, and 9). (b) $\ln(n_l)$ as a function of $\ln(T_t - T)$ for coverages of 0.24 molecules/Å^2 (diamonds) and 0.32 molecules/Å^2 (squares) layers. The dashed line corresponds to the best logarithmic fit to the data. The dotted line corresponds to a power law with exponent $-\frac{1}{3}$, Eq. (12).

The dashed curve shows the best fit to the data and is not linear. The dotted line shows the expected behavior if the data were to follow the power law

$$n_l \propto (T_t - T)^{-1/3} . \quad (12)$$

The thickness of the surface-melted liquid layer increases logarithmically until the layer has completely melted. For surface coverages 0.24 and 0.32 molecules/Å^2 ($n_l = 3.2$ and 4.2 layers) this occurs at $T = 46.5$ K and 48 K, respectively. The logarithmic dependence will be discussed in a following section.

3D γ oxygen is cubic with eight molecules per unit cell, and is stable from 43.8 to 54.4 K.[34] Throughout this temperature range no film phase occurs which is similar to 3D γ oxygen. We conclude that both the beta phase and the liquid phase wet graphite more strongly than γ oxygen. Complete wetting by the γ phase is therefore prevented. This is apparently due to the attractive nature of the substrate, and so a preference for the higher density β phase.

It has been previously shown that liquid oxygen completely wets graphite.[35] To verify that γ oxygen does not wet graphite, and to investigate the wetting behavior of β oxygen, we carried out scans at fixed temperatures with increasing surface coverage. Figure 6 shows a series of scans carried out at 49.5 K in the fluid film regime for four surface coverages ranging from 0.24 to 0.9 molecules/Å^2 (the equivalent of three to twelve liquid layers). All coverages greater than 0.32 molecules/Å^2 (~four liquid layers) show the 3D γ phase coexisting

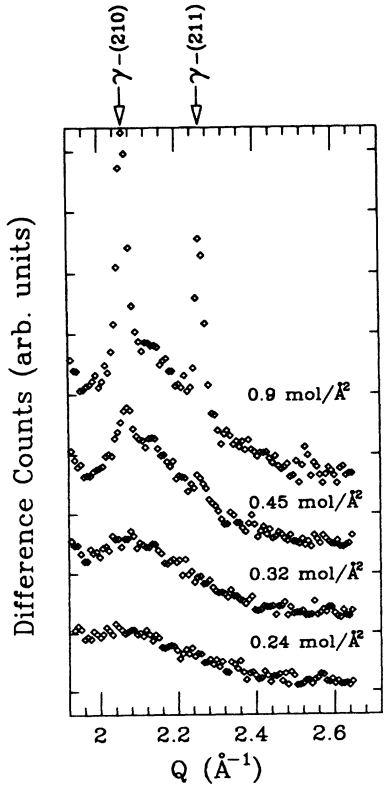

FIG. 6. Diffraction scans recorded at 49.5 K for coverages ranging from 0.24 to 0.9 molecules/Å^2. Bulk γ peaks appear at coverages greater than 0.32 molecules/Å^2.

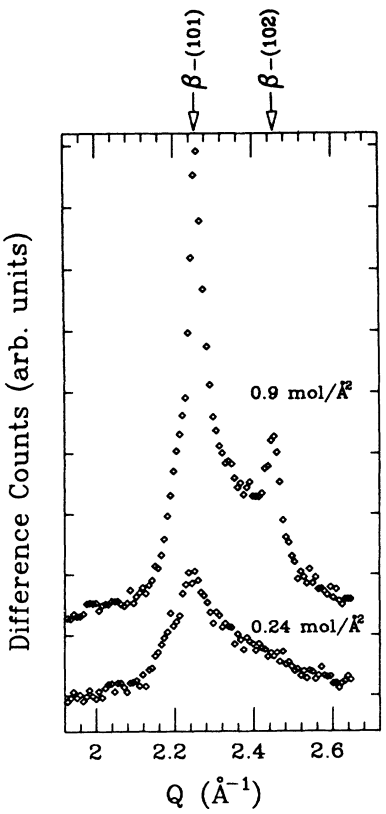

FIG. 7. Diffraction scans recorded at 34.5 K for coverages of 0.24 and 0.9 molecules/Å^2, along with the locations of the bulk β peaks.

with the fluid film phase, an indication of incomplete wetting by the γ phase. It is interesting to note that as the amount of γ solid increases, the liquid present also increases. This is an indication that the surface of the γ oxygen may also be melted.

Figure 7 shows two scans recorded in the 2D solid regime at 34.5 K at surface coverages of 0.24 and 0.9 molecules/Å^2 (the equivalent of two to eight solid layers). The lower coverage is a 2D solid film. The fit of this scan is shown in Fig. 4(b). At the higher coverage it is not obvious that a 3D solid crystallite is coexisting with a 2D film. Indeed, the film parameters at this temperature are so close to those of the bulk solid that it is possible that the film completely wets graphite at this temperature. We know of no experimental evidence to the contrary.

We have not fit the film scan shown in Fig. 3 for 0.32 molecules/Å^2 at 46.5 K. This scans consists of a surface-melted film line shape and an additional peak corresponding to the 3D γ phase. The appearance of the bulk γ peak at this temperature is consistent with our conjecture that both the liquid and β phases wet graphite more strongly. The coexistence of 2D and 3D phases at 46.5 K is indicative of incomplete wetting. 3D peaks are observed at neither higher nor lower temperatures for this particular coverage. This implies that as the temperature tends towards regimes where either the bulk liquid or β phases are stable, thicker 2D film phases are able to form.

VI. DISCUSSION

Zhu and Dash[17] have studied surface melting in the system Ar on graphite via heat-capacity measurements and have observed a power law dependency for the melted surface layer. In contrast, our data for oxygen films exhibit a logarithmic dependence on temperature. The argon films studied by Zhu and Dash were much thicker than those studied here, and provide a good indication of how 3D solid argon should melt. Our results lend no insight to the melting of 3D γ oxygen since its formation was preempted by the combined efforts of the liquid and β phases. It is quite possible that if surface melting occurs in γ oxygen, the thickness of the melted layer will be described by a power law.

For the case at hand, we are observing surface melting of a thin film similar in structure to β oxygen. The logarithmic dependence of the liquid thickness is consistent with that predicted[22] for surface melting in semi-infinite systems with short-range effective interactions. Short-ranged interactions may dominate here due to the very limited film thicknesses involved.

It is apparent that both liquid and β oxygen wet graphite more strongly than the γ phase, so that oxygen will not wet graphite at any temperature where γ is the stable 3D phase. This being the case, it is conceivable that oxygen may exhibit multiple transitions from wetting to incomplete wetting at 54.4 K, from incomplete to complete wetting near 43.8 K, and back to incomplete wetting at an even lower temperatures where oxygen is known to form 3D crystallites. While this remains conjecture, it is certainly true that the film growing at 34.5 K has a nearly identical structure to the bulk phase it must eventually coexist with.

VII. SUMMARY

We have studied the melting behavior of bilayer and trilayer oxygen films on graphite and observe a compound film in the temperature range 39–47 K which results from surface melting. The solid component of this film displays diffraction patterns essentially identical to those of true solid monolayers and bilayers and has structure similar to that of the bulk β phase of oxygen. The quantity of surface-melted liquid increases as $\ln(T_t - T)$, consistent with surface melting predictions for short-ranged interactions. The data indicate that multiple wetting transitions may be present in this system.

ACKNOWLEDGMENTS

We wish to thank P. Convert of Institut Laue-Langevin for his invaluable assistance throughout the run of these experiments and J. Bouzidi for help in collecting the data. We gratefully acknowledge useful discussions with J. Suzanne, P. Vora-Purohit, and H. Taub. J. G. Dash is especially thanked for his comments and careful reading of our manuscript. This work was supported in part by a grant from PPG Industries Foundation through Research Corporation, in part by the National Science Foundation–Low Temperature Physics—Grant No. DMR 8657211 (R.C. and J. K.), and in part by Centre National de la Recherche Scientifique (J.P.C.).

*Permanent address: Département de Physique, Case 901, Faculté des Sciences de Luminy, 13288 Marseille, Cédex 9, France.

[1]J. G. Dash, *Films on Solid Surface* (Academic, New York, 1975).
[2]R. Marx, Phys. Rep. **125**, 1 (1985).
[3]P. A. Heiney, P. W. Stephens, S. G. J. Mochrie, J. Akimitsu, R. J. Birgenau, and P. M. Horn, Surf. Sci. **125**, 539 (1983).
[4]D. D. Awschalom, G. N. Lewis, and S. Gregory, Phys. Rev. Lett. **51**, 586 (1983).
[5]S. C. Fain, Jr., M. F. Toney, and R. D. Diehl, in *Proceedings of the Ninth International Vacuum Congress and Fifth International Conference on Solid Surfaces,* edited by J. L. de Segovia (Imprenta Moderna, Madrid, 1983), pp. 129–137.
[6]J. Stoltenberg and O. E. Vilches, Phys. Rev. B **22**, 2920 (1980).
[7]J. P. McTague and M. Nielsen, Phys. Rev. Lett. **37**, 596 (1976).
[8]M. Nielsen and J. P. McTague, Phys. Rev. B **19**, 3096 (1979).
[9]C. E. Bartosch and S. Gregory, Phys. Rev. Lett. **54**, 2513 (1985).
[10]M. Drir and G. B. Hess, Phys. Rev. B **33**, 4758 (1986).
[11]M. F. Toney and S. C. Fain, Jr., Phys. Rev. B **36**, 1248 (1987).
[12]U. Kobler and R. Marx, Phys. Rev. B **35**, 9809 (1987).
[13]M. Morishige *et al.*, Surf. Sci. **192**, 197 (1988).
[14]M. Bienfait, J. L. Seguin, J. Suzanne, E. Lerner, J. Krim, and J. G. Dash, Phys. Rev. B **29**, 983 (1984), see also Refs. 6, 9, and 15.
[15]J. Krim, J. P. Coulomb, and J. Bouzidi, Phys. Rev. Lett. **58**, 583 (1987).
[16]J. W. Frenken and J. K. van der Veen, Phys. Rev. Lett. **54**, 134 (1985).
[17]D. M. Zhu and J. G. Dash, Phys. Rev. Lett. **57**, 2959 (1986).
[18]M. Bienfait, Europhys. Lett. **4**, 79 (1987).
[19]J. K. Kristensen and R. M. J. Cotterill, Philos. Mag. **36**, 437 (1977).
[20]J. Q. Broughton and G. H. Gilmer, J. Chem. Phys. **79**, 5119 (1983).
[21]R. Lipowsky and G. Gompper, Phys. Rev. B **29**, 5213 (1984).
[22]R. Lipowsky, Phys. Rev. Lett. **49**, 1575 (1982).
[23]R. Lipowsky and W. Speth, Phys. Rev. B **28**, 3982 (1983).
[24]R. Pandit and M. E. Fisher, Phys. Rev. Lett. **51**, 1772 (1983).
[25]C. Ebner, Phys. Rev. B **28**, 2890 (1983).
[26]M. Bienfait, Surf. Sci. **162**, 411 (1985).
[27]J. Krim, J. G. Dash, and J. Suzanne, Phys. Rev. Lett. **52**, 640 (1984).
[28]Y. Larher, F. Angerand, and Y. Maurice, J. Chem. Soc., Faraday Trans. 1 **83**, 3355 (1987).
[29]J. K. Kjems, L. Passell, H. Taub, J. G. Dash, and A. D. Novaco, Phys. Rev. B **13**, 1446 (1976).
[30]J. Z. Larese, M. Harada, L. Passell, J. Krim, and S. Satija, Phys. Rev. B **37**, 4735 (1988).
[31]G. Herzberg, *Spectra of Diatomic Molecules* (Van Nostrand, Princeton, 1970).
[32]J. P. Coulomb, D. Etat Sci. thesis, University of D'Aix Marseille II, 1981.
[33]W. Ruland and H. Tompa, Acta Crystallogr. A **24**, 93 (1968).
[34]G. C. De Fotis, Phys. Rev. B **23**, 4714 (1981).
[35]Drir and Hess (Ref. 10) observe liquid oxygen to "almost wet" graphite in that a thick film of 12 or more layers is able to form. For this discussion we will not disinguish between complete wetting and "thick film" formation.